Acta Cryst. (1980). B36, 1997–2000

$\mathrm{RbAlF_4}$: Structure of Its β Metastable Form and Description of the Mechanism of Its Irreversible and Topotactic Phase Transition $\beta \rightarrow \alpha$

By J. L. Fourquet, F. Plet and R. De Pape

Laboratoire des Fluorures et des Oxyfluorures Ioniques, Faculté des Sciences du Mans, Equipe de Recherche associée au CNRS n° 609, route de Laval, 72017 Le Mans CEDEX, France

(*Received* 18 *February* 1980; *accepted* 24 *March* 1980)

Abstract

Single crystals of β-$\mathrm{RbAlF_4}$ were prepared by hydrothermal synthesis. The cell is tetragonal [a = 11·666 (5), c = 12·551 (6) Å, $I\bar{4}c2$, Z = 20]. Final R = 0·0242 (R_w = 0·0178). The structure is closely related to that of tetragonal tungsten bronze and is built from two $[\mathrm{AlF_{4/2}F_2^-}]_\infty$ layers of $\mathrm{AlF_6}$ octahedra, connected by four corners, in the (001) plane. The Rb atoms are located between the layers in the vicinity of all the square and pentagonal holes. At 588 K, the crystals transform into the stable α form by an irreversible, non-destructive and topotactic phase transition, which is explained by a concerted $\pi/4$ rotation, around the c axis, of four-octahedra groups. This transformation illustrates experimentally the theoretical concept of bounded rotation faults previously discussed and employed to demonstrate the relation between the perovskite and the tetragonal tungsten bronze networks.

Introduction

Tetragonal $M^{\mathrm{I}}\mathrm{AlF_4}$ compounds (M^{I} = K, Rb, $\mathrm{NH_4}$, Tl) have been described (Brosset, 1938). They are built from $[\mathrm{AlF_{4/2}F_2^-}]_\infty$ layers in which $\mathrm{AlF_6}$ octahedra are connected by four corners in the (001) plane. The structural type is $\mathrm{TlAlF_4}$ [a_0 = 3·616 (3), c_0 = 6·366 (3) Å, $P4/mmm$, Z = 1]. During a reinvestigation of this series, we have shown (Fourquet, Plet, Courbion, Bulou & De Pape, 1979) that in fact these phases present small distortions from the aristotype. The relation of the space groups, at room temperature, is shown in Fig. 1. The crystallographic characteristics of the room-temperature-stable form of $\mathrm{RbAlF_4}$, which is hereafter referred to as the α form, are: space group $P4/mbm$, Z = 2, a = 5·125 (2), c = 6·283 (2) Å, ρ_o = 3·80 (1), ρ_c = 3·792 Mg m^{-3}.

We report here the structure of a new form that we call β-$\mathrm{RbAlF_4}$.

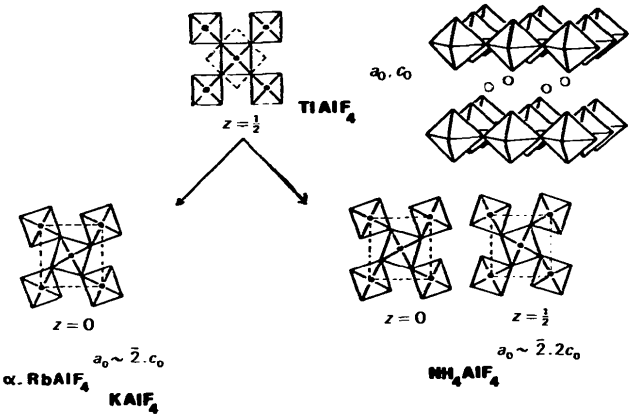

Fig. 1. Relation of the structures of the $M^{\mathrm{I}}\mathrm{AlF_4}$ series and that of $\mathrm{TlAlF_4}$.

Preparation

Single crystals of β-$\mathrm{RbAlF_4}$ were prepared by hydrothermal synthesis in a medium of hydrofluoric acid (Plet, Fourquet, Courbion, Leblanc & De Pape, 1979). Crystals of both the α and β forms grow simultaneously at T = 573 K under 180 MPa; crystals of the α form are transported to the top of the tube, while those of the β form are deposited in the lower part.

Crystals of β-$\mathrm{RbAlF_4}$ are small, colourless square plates; they do not show the lamellar aspect exhibited by those of the α form, so they can be easily separated. Standard chemical analysis confirms the formulation.

Crystallographic study and data collection

Laue photographs reveal that β-$\mathrm{RbAlF_4}$ belongs to the $4/mmm$ Laue group. The absences hkl with $h + k + l \neq 2n$ and $h0l$ with $h \neq 2n$ lead to three possible space groups, $I4/mcm$, $I\bar{4}c2$, $I4cm$. The cell parameters were determined with the Nonius CAD-4 automated four-circle diffractometer used for the data collection. The

0567-7408/80/091997-04$01.00

density was measured by flotation: ρ_o = 3·66 (1) Mg m^{-3} which is consistent with Z = 20 (ρ_c = 3·664 Mg m^{-3}).

The data collection was performed with graphite-monochromatized Mo $K\alpha$ radiation from a single crystal with boundary faces defined by $\pm\{110\}$, $\pm\{001\}$ and $\pm\{1\bar{1}0\}$, which was 0·248 × 0·135 × 0·194 mm. 3005 reflections satisfying the conditions $-16 < h, k < 16$ and $0 < l < 16$ were explored with an ω–2θ scanning technique. After correction of Lorentz–polarization and absorption effects (μ = 14·289 mm^{-1}), the data were averaged and reduced to 433 independent observations with $\sigma(I)/I < 0{\cdot}333$.

Structure resolution

All calculations were performed with *SHELX* (Sheldrick, 1976). In the absence of any information about the structure, we first tried direct methods with the option *TANG* in the more symmetric space group I4/*mcm*. The best five resulting solutions were evaluated by a criterion based upon the shortest interatomic distances, which were compared to a standard Al—F = 1·80 Å. Atomic coordinates and anisotropic thermal parameters were refined by full-matrix least squares to R = 0·0658 (R_w = 0·0657). Calculations were then made for the two non-centrosymmetric groups which gave R = 0·0242 and R_w = 0·0178 for $I\bar{4}c2$ and R = 0·0233 and R_w = 0·0174 for $I4cm$. The Hamilton-ratio values first discard $I4/mcm$, and finally the value $\mathscr{R}_{19,354,0\cdot005}$ = 1·064, compared to $R_w(I\bar{4}c2)/R_w(I4cm)$ = 1·0229, indicates that $I\bar{4}c2$ is the most probable space group at the 0·995 confidence level. Table 1 gives the final atomic parameters.*

Description of the structure

The structure is built by two $[\mathrm{AlF}_{4/2}\mathrm{F}_2^-]_\infty$ quasi-planar layers of AlF$_6$ octahedra, connected through four corners, in the (001) plane. Fig. 2 shows projections along c of the (001) planes of the two layers (at z = 0 and $\frac{1}{2}$); they are similar to the familiar tetragonal tungsten bronze structure. Rb atoms are located on both sides of all the square and pentagonal holes left in the layers.

There are two different kinds of AlF$_6$ octahedra (Table 2), the shortest Al—F distances lying in both cases along c. Rb—F distances are listed in Table 3 and Fig. 3 shows the environment of the two kinds of Rb atoms. Rb(1) has an almost regular (8 + 8) environment, while Rb(2) exhibits a more complex coordination with 13 neighbours. In the classical tetragonal tungsten bronze, $A^1_xMX_3$, A^1 can occupy dodecahedral cavities (CN 12) and pentagonal sites (CN 15). The changes in the Rb coordination numbers in this structure are due to the separation of the layers perpendicular to c: this process leaves more room for the Rb atoms.

Finally, if the TlAlF$_4$ structure can be described as a disconnected perovskite along c, β-RbAlF$_4$ can be seen as a disconnected tetragonal tungsten bronze along the

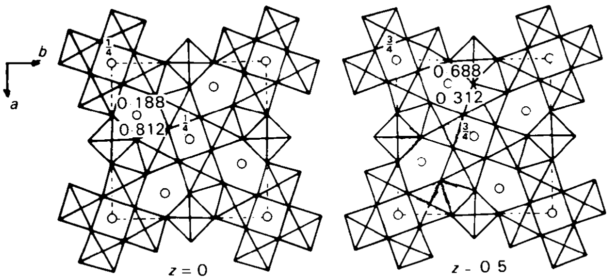

Fig. 2. Idealized projection of the structure of β-RbAlF$_4$ on the z = 0 and $\frac{1}{2}$ levels.

Table 1. *Atomic coordinates and* $B_{\rm eq}$ *of* β-RbAlF$_4$ *with e.s.d.'s in parentheses*

The isotropic extinction parameter x (Sheldrick, 1976) takes the value 122 (3) × 10^{-5}.

	Site	x	y	z	$B_{\rm eq}$ (Å^2)
Rb(1)	4(a)	0	0	$\frac{1}{4}$	1·465
Rb(2)	16(i)	0·3415 (2)	0·8404 (2)	0·6881 (0)	1·894
Al(1)	4(d)	$\frac{1}{2}$	0	0	0·610
Al(2)	16(i)	0·7926 (1)	0·0763 (1)	0·0007 (7)	0·621
F(1)	16(i)	0·3445 (2)	0·0011 (2)	0·0015 (11)	1·279
F(2)	16(i)	0·1419 (2)	0·0667 (2)	0·0012 (16)	1·529
F(3)	16(i)	0·0777 (10)	0·2061 (9)	0·1385 (10)	2·013
F(4)	16(i)	−0·0801 (9)	−0·2111 (9)	−0·1400 (8)	1·052
F(5)	8(h)	0·2184 (2)	−0·2816 (2)	$\frac{1}{2}$	1·260
F(6)	8(g)	0	$\frac{1}{2}$	0·1379 (3)	1·521

Table 2. *The* Al—F *distances* (Å) *in octahedral sites*

F atoms are denoted by two numbers: the first refers to the type of F atom in Table 1, the second characterizes the coordinates of equivalent positions of the Wyckoff position; *e.g.*, for 16(i): x,y,z; $\bar{x},\bar{y},\bar{z}$; *etc.*

Al(1) octahedra				
Al(1)—F(11)	1·814 (2)	Al(1)—F(64)	1·731 (3)	(along c)
Al(1)—F(12)		Al(1)—F(63)		
Al(1)—F(17)				
Al(1)—F(18)		Mean Al(1)—F	1·786	
Al(2) octahedra				
Al(2)—F(12)	1·837 (2)	Al(2)—F(35)	1·747 (15)	(along c)
Al(2)—F(25)	1·811 (2)	Al(2)—F(46)	1·749 (13)	
Al(2)—F(22)	1·835 (2)	Al(2)—F(51)	1·870 (2)	
		Mean Al(2)—F	1·808	

---

* Lists of structure factors and anisotropic thermal parameters have been deposited with the British Library Lending Division as Supplementary Publication No. SUP 35292 (4 pp.). Copies may be obtained through The Executive Secretary, International Union of Crystallography, 5 Abbey Square, Chester CH1 2HU, England.

Table 3. *The* Rb—F *distances* (Å)

Rb(1) polyhedron		Rb(2) polyhedron	
Rb(1)–F(31)	2·926 (11)	Rb(2)–F(61)	2·699 (2)
Rb(1)–F(32)		Rb(2)–F(44)	2·787 (10)
Rb(1)–F(37)		Rb(2)–F(36)	2·854 (12)
Rb(1)–F(38)		Rb(2)–F(14)	2·984 (11)
		Rb(2)–F(15)	3·006 (11)
Rb(1)–F(45)	2·974 (10)	Rb(2)–F(51)	3·108 (2)
Rb(1)–F(46)		Rb(2)–F(46)	3·156 (10)
Rb(1)–F(43)		Rb(2)–F(34)	3·187 (11)
Rb(1)–F(44)		Rb(2)–F(31)	3·231 (11)
		Rb(2)–F(48)	3·240 (10)
Rb(1)–F(28)	3·619 (17)	Rb(2)–F(52)	3·414 (3)
Rb(1)–F(27)		Rb(2)–F(24)	3·479 (13)
Rb(1)–F(22)		Rb(2)–F(25)	3·486 (13)
Rb(1)–F(21)			
Rb(1)–F(24)	3·645 (17)		
Rb(1)–F(23)			
Rb(1)–F(25)			
Rb(1)–F(26)			

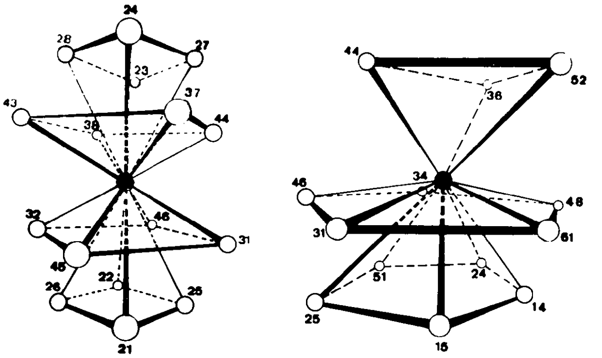

(*a*) (*b*)

Fig. 3. Environment of the Rb atoms. The black circle is Rb^+. F^- ions are labelled according to Table 3. (*a*) and (*b*) show the Rb(1) and Rb(2) polyhedra respectively.

same axis: in both cases different $[AlF_{4/2}F_2^-]_\infty$ layers of AlF_6 octahedra are produced.

The $\beta \rightarrow \alpha$ phase transition

When crystals of the β form are heated under argon at atmospheric pressure for 2 h at temperatures >588 ± 10 K, they become opalescent and are topotactically transformed into crystals of the α form without destruction of the faces and without any twinning. The process is irreversible and there is no detectable DTA peak before 846 K, which is the α-$RbAlF_4$ melting point. The transformation has been checked by an X-ray diffraction study of several heated crystals of the β form: Laue and Buerger films are strictly similar to those produced by α-form crystals.

Figs. 4 and 5 show the proposed mechanism involved in this phase transition. The α-$RbAlF_4$ network is built by a 20° clockwise rotation of the Al(1)F_6 octahedra around the [001] direction, and simultaneously by a π/4 concerted rotation around the fourfold axis of Al(2)F_6 four-octahedra groups. These movements are consistent with the *I* mode, and the transformation produces the same network at the $z = 0$ and $\frac{1}{2}$ levels, so the new cell has a c_α parameter which is half c_β: $c_\alpha = 6{\cdot}283\ (2)$ Å $\simeq c_\beta/2$ (Fig. 5).

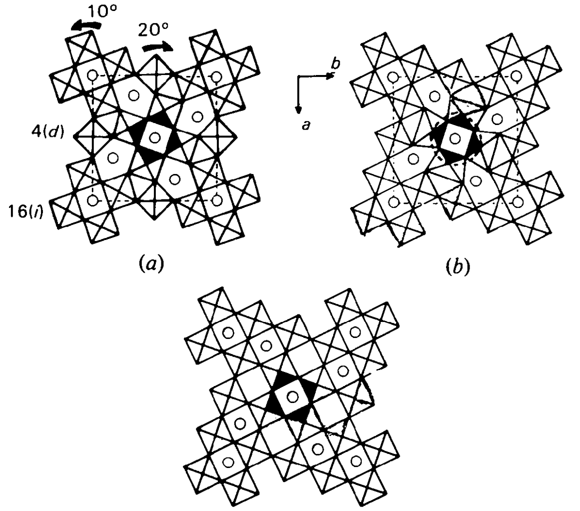

(*a*) (*b*)

(*c*)

Fig. 4. Representation of the mechanism of the phase transition at the $z = \frac{1}{2}$ level. On (*a*) the arrows show the rotation of the Al[4(*d*)]F_6 octahedra and of the group of four Al[16(*i*)]F_6 octahedra around the [001] direction. In black, we have shown the Al_4F_{12} group which really undergoes the π/4 rotation, in which Al exhibits transitorily a coordination number of 4 (see *b*). (*c*) shows the result of the transformation: a layer with a perovskite network.

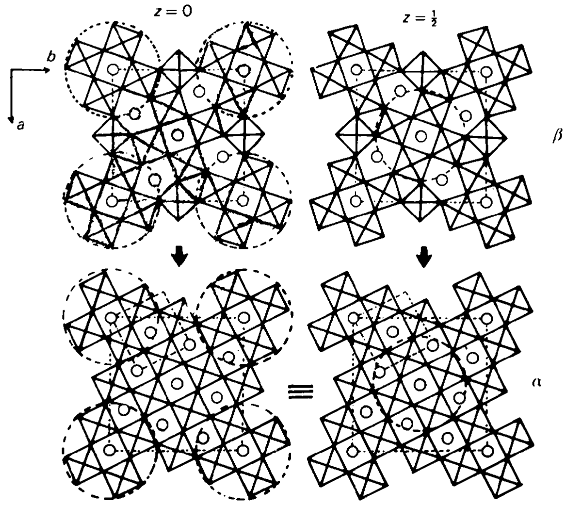

Fig. 5. Formation of the α-$RbAlF_4$ network from the $z = 0$ and $\frac{1}{2}$ levels of the β-$RbAlF_4$ structure. The dotted circles show the four-octahedra groups which are rotated by π/4 to form the same layer of a perovskite-type network. The α and β unit cells are represented.

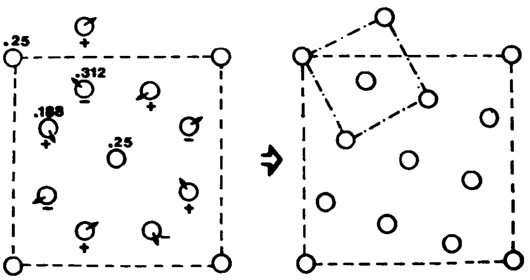

Fig. 6. Cooperative displacements of the Rb$^+$ ions in the transformation, represented here near the $z = 0{\cdot}25$ level. Upward (+) and downward (−) movements are shown. In the right part, all the Rb atoms are at $z = 0{\cdot}25$. α(– – –) and β (–·–) unit cells are represented.

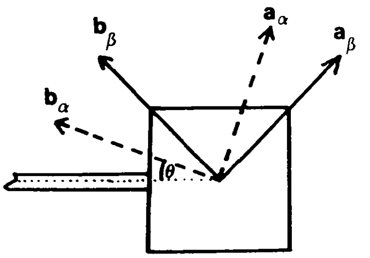

Fig. 7. Relation between the axes of the α and β forms in a single crystal. The theoretical value of the angle between a_α and a_β is $\pi/4 - \theta = 26{\cdot}56°$.

Fig. 6 shows the reorganizing of the Rb atoms: those at $z = \frac{1}{4}$ and $\frac{3}{4}$ are motionless, while the others undergo 1·14 Å shifts.

The unit cells of the α and β forms are related as follows:

$$a_\beta \simeq 2a_\alpha - b_\alpha$$
$$b_\beta \simeq 2b_\alpha + a_\alpha$$
$$c_\beta \simeq 2c_\alpha.$$

The mutual orientation of the two unit cells has been confirmed by the measurement of the rotation angle θ around c (Fig. 7) necessary to superpose the Laue photograph of a transformed crystal of the β form and one of a crystal of the α form, fixed on its b_α axis. The experimental tilt θ is 20°, which is consistent with the theoretical value of 18·72°.

The mechanism proposed here is an experimental illustration of the concept of a bounded rotation fault or rotatory stacking fault previously described (Bursill & Hyde, 1972; Hyde & O'Keeffe, 1972; Iijima & Allpress, 1974; Iijima, 1978) to relate the perovskite network to various tunnel structures. Here, such a mechanism involves a very low energy, the propagation of the defect being very easy in this layered structure.

The small volume change $\Delta V/V$ observed, −3·39%, and the similarity of the Coulombic parts of the electrostatic energies (−7923 kJ mol^{-1} for α and −7879 kJ mol^{-1} for β) indicate that we have probably observed for the first time a perfect topotactic transformation, *i.e.* the integrity of the crystal is kept, and it is propagated from one point so that no twinning is encountered.

We are undertaking high-resolution electron-microscopy observations.

We thank Professor Hardy (Poitiers) for the data-collection facilities and Mrs Mercier (CNRS) who performed the chemical analysis and DTA measurements.

References

Brosset, C. (1938). *Z. Anorg. Allg. Chem.* **239**, 301.

Bursill, L. A. & Hyde, B. G. (1972). *Nature* (*London*) *Phys. Sci.* **240**, 122–124.

Fourquet, J. L., Plet, F., Courbion, G., Bulou, A. & De Pape, R. (1979). *Rev. Chim. Minér.* **16**, 490–500.

Hyde, B. G. & O'Keeffe, M. (1972). *Acta Cryst.* A**29**, 243–248.

Iijima, S. (1978). *Acta Cryst.* A**34**, 922–931.

Iijima, S. & Allpress, J. G. (1974). *Acta Cryst.* A**30**, 22–29.

Plet, F., Fourquet, J. L., Courbion, G., Leblanc, M. & De Pape, R. (1979). *J. Cryst. Growth*, pp. 699–702.

Sheldrick, G. M. (1976). *SHELX*. Program for crystal structure determination. Univ. of Cambridge, England.